UCRL-JRNL-228623

LAWRENCE
LIVERMORE
NATIONAL
LABORATORY

Initiation Pressure Thresholds from Three Sources

P. C. Souers, P. Vitello

March 4, 2007

Propellants, Explosives, Pyrotechnics

Disclaimer

This document was prepared as an account of work sponsored by an agency of the United States Government. Neither the United States Government nor the University of California nor any of their employees, makes any warranty, express or implied, or assumes any legal liability or responsibility for the accuracy, completeness, or usefulness of any information, apparatus, product, or process disclosed, or represents that its use would not infringe privately owned rights. Reference herein to any specific commercial product, process, or service by trade name, trademark, manufacturer, or otherwise, does not necessarily constitute or imply its endorsement, recommendation, or favoring by the United States Government or the University of California. The views and opinions of authors expressed herein do not necessarily state or reflect those of the United States Government or the University of California, and shall not be used for advertising or product endorsement purposes.

Initiation Pressure Thresholds from Three Sources

P. Clark Souers* and Peter Vitello

Energetic Materials Center, Lawrence Livermore National Laboratory, Livermore, CA 94550 (USA)

*Corresponding author; e-mail: souers1@llnl.gov

Abstract

Pressure thresholds are minimum pressures needed to start explosive initiation that ends in detonation. We obtain pressure thresholds from three sources. Run-to-detonation times are the poorest source but the fitting of a function gives rough results. Flyer-induced initiation gives the best results because the initial conditions are the best known. However, very thick flyers are needed to give the lowest, asymptotic pressure thresholds used in modern models and this kind of data is rarely available. Gap test data is in much larger supply but the various test sizes and materials are confusing. We find that explosive pressures are almost the same if the distance in the gap test spacers are in units of donor explosive radius. Calculated half-width time pulses in the spacers may be used to create a pressure-time curve similar to that of the flyers. The very-large Eglin gap tests give asymptotic thresholds comparable to extrapolated flyer results. The three sources are assembled into a much-expanded set of near-asymptotic pressure thresholds. These thresholds vary greatly with density: for TATB/LX-17/PBX 9502, we find values of 4.9 and 8.7 GPa at 1.80 and 1.90 g/cm^3, respectively.

Keywords: initiation, threshold, run-to-detonation, gap tests, critical energy

There is considerable evidence that a certain pressure threshold must be exceeded to start explosive initiation that ends in detonation. The traditional flyer method is represented by limited data. We here consider three sources of data and compare the results.

1 Flyer Data

The modern way of studying threshold initiation is to shoot a metal or plastic flyer of known thickness and velocity at an explosive. Various parameters are tried, some of which cause detonation and some do not until an approximate 50% detonation point is reached. The flyer parameters are converted into inert explosive instant-of-impact pressures, P, and pulse lengths, τ, using impedance calculations. The P-τ curves, which generally have too few points, especially at low pressures, have to be analyzed with some format, which we now consider.

Walker and Wasley defined the critical energy, E_{cr}, for threshold initiation, which is derived using [1,2]

$$E_{cr} = Pu_p\tau\,, \tag{1}$$

where u_p is the particle velocity. We then substitute the conservation equation

$$P = \rho_o U_s u_p \tag{2}$$

to get their equation

$$E_{cr} = \frac{P^2 \tau}{\rho_o U_s}, \tag{3}$$

where ρ_o is the initial explosive density and U_s is the wave velocity in the unreacted explosive. E_{cr} is the amount of energy per unit area of the flyer crossing into the explosive. Walker and Wasley hoped this would be constant for each explosive, but de Longueville experimentally showed that it was not for Comp B, NM, RDX/pb, and liquid TNT [3]. He found it was constant for HMX/nylon and possibly for two granular RDX's. At our laboratory, LX-17 was found to not be constant, but excuses were made to keep Eq. (3) alive.

James presented a theory with an asymptotic threshold for E_{cr}, which he interprets as a trigger energy that does not affect the succeeding stages of run-to-detonation [4]. At low pressures, he defines a particle velocity-squared asymptotic threshold, u_{po}^2, given by

$$u_p^2 = \frac{E_{cr}}{\rho_o U_s \tau} + u_{po}^2 \tag{4}$$

so that

$$E_{cr}(u_p^2) = \rho_o U_s \tau \left(u_p^2 - u_{po}^2 \right). \tag{5}$$

We may define the corresponding asymptotic pressure threshold P_o from this as being

$$P_o = \rho_o U_{so} u_{po}. \tag{6}$$

The use of velocity-squared, rather than pressure, which has consistently been popular in hydro-code models, is reminiscent of Roth, who suggested a similar approach in the early days of run-to-detonation measurements [5].

At high pressures (considerably above C-J), there is also a time threshold somewhere around 0.01 μs. The importance of the James theory is that: first, he establishes definitely the existence of an initiation threshold, and second, he brings back the critical energy as a real constant.

Because the reactive flow burn rates in our hydro-codes use a pressure ignition threshold, we try a different approach. Eq. (2) above must be true because there is a shock wave there, whether it triggers detonation or not. Eq. (3) also holds as a measure of the energy flowing through, but we can define some part of it as triggering the explosive. The critical energy becomes

$$E_{cr}(P) = \frac{(P - P_o)^2 \tau}{\rho_o U_s} \tag{7}$$

which has the look of Eq. (3). This can be turned into

$$E_{cr}(P) = \frac{\rho_o}{U_s}(U_s u_p - U_{so} u_{po})^2 \tau\,, \tag{8}$$

which is different from Eq. (5). We use Eq. (6) in reverse to get u_{po} as a constant.

A plot of P versus τ forms the 50% probable-detonation initiation curve. Thin pulses require high pressures and vice versa. For large τ, P approaches an asymptotic low value of P_o, and it is this value that is used in modeling. If P_o is almost zero, as would occur for an ideal explosive, then Eq. (7) becomes Eq. (3), as was found with three of de Longueville's experiments.

Finding the asymptotic pressure directly is difficult, but LeRoy Green tried this with LX-17 in 1978 [6]. Steel sabots of 155 mm diameter were fired into LX-17-0 (called RX-03-BB then) samples of nominal 1.90 g/cm^3 density of 152.4 mm diameter and 101.6 mm length. Manganin gauges of 0.25 mm thickness and 6 mm diameter were placed inside the LX-17 at distances of 12.7, 38.1, 63.5 and 88.9 mm. From the observed explosion intensity, Green thought that a 1.1 mm/μs flyer with a thickness of 36 mm caused a reaction that continued to build and would have detonated if the sample had been large enough. A second shot at 1.0 mm/μs with a 50.8 mm-thick flyer caused no reaction. These may be converted to a 14.4 μs pulse at 7.5 GPa for the shot that started to react and 20.5 μs and 6.6 GPa for the shot that did not. So, P_o may be about 7.5 GPa but it is difficult to be sure.

In the 1980's, detonation was assigned by the flashing of aluminum silicofluoride. However, this was found to occur at only 2.9 GPa, so that some results may not be true detonation [7]. In a recent return to this method, a steel witness plate was used for this reason [8].

2 Run-to-Detonation Times (Pop Plots)

Run-to-detonation experiments are done differently from flyer initiation experiments. The flyers are thin, so much so that they are bent back at the edges in flight. However, the run-time experiments are done with massive 25-50 mm-long sabots that do not deform and are so thick that the pressure is held constant over the entire run-to-detonation of 10-20 μs length. The run-time experiments have large radii so that side rarefactions have no effect on the times, which are measured with on-axis gauges. The run-time experiments are measured well above the P-τ 50% line and are guaranteed to detonate. Yet, when the two are plotted together, both appear to be approaching an asymptotic pressure.

We also note that the pressure in the initiation region does not stay at the initial impact value of P_i but gradually increases with time, t, so that

$$P \approx P_i + at\,, \tag{9}$$

where a is a constant. Because of the form of Eq. (7), we will write our initiation rate equation in terms of $(P - P_o)^2$. Analytically, we must account for the slow rise in the pressure as the run-to-detonation continues, so we have

$$\frac{dF}{dt} = G\left[(P_i - P_o) + at\right]^2 (1 - F)\,, \tag{10}$$

where G is the rate constant and F is the burn fraction. We will integrate this to a final burn fraction F_e and a run-to-detonation time, t_e. We collect the pressure terms on the right and get

$$\frac{-ln(1-F_e)}{G} - \frac{a^2 t_e^3}{3} = (P_i - P_o)^2 t_e + a(P_i - P_o) t_e^2\,. \tag{11}$$

Just as we did with critical energy, we have to set something- the left side of Eq. (11) - constant in order to continue. We calculate the right side using the data and various a and P_o values until we get constant results. We also estimate that a $\approx$ 4 GPa from the few run-times we have done with our model on LX-17. We find that as we increase the constant a in the fitting process, that P_o becomes constant (usually with a = 4) for that explosive, and this is the number we take.

3 Gap Test Data

The gap test appears to have originated first at the U. S. Bureau of Mines in 1931 [9] and was studied in Canada by Herzberg and Walker in the 1940's [10, 11]. Los Alamos (LANL) perhaps first used gap tests as a production method to determine the sensitivity of explosives. The test consists of a cylindrical donor explosive that sends a shock wave through an inert spacer material into the acceptor explosive of interest. The spacer thickness is varied from shot to shot until the 50% point of causing detonation, as determined from the results in a steel witness plate at the end of the cylinder. We consider the results in terms of either full detonation or not. One criticism of the gap test is that it does not represent true shock initiation, but initiation is actually caused by surface waves [12]. This comes from a paper that calculates low amplitude oscillations in vibrating membranes using linear mathematics [13]. A detonation, however, is a non-linear event which why code modeling, with all its imperfections, is used to represent it, and shall proceed with the assumption that shock compression is the dominant phenomenon. A second criticism is that low velocity detonation could be present [14]. This phenomenon is called a non-detonative explosion in the American literature, and while real, it appears to require special conditions to happen [15]. It might be there by accident in some of the many gap tests, but there is no way to sort them out.

The geometries of the various tests are listed in Table 1 [16-25]. The flyer method is at the top, and the gap tests are listed in descending order of how much they usually deviate from the flyer results. In general, the farther down, the older is the test, so that brass was the first spacer, followed by aluminum and now Lucite. As time went by, the size of the parts increased and more expensive confinement of the acceptor was added. The Air Force at Eglin AFB is currently running gap tests with the largest sizes ever used. The U. S. Navy's Large Scale Gap Test has the largest inventory of data.

In Table 1, the U. S. Navy is NSWC, SSGT means small-scale gap test and LSGT is the large scale gap test. In the lower quantity tests, MGT is the modified gap test, IHEGT is for insensitive high explosives and ELSGT is the Eglin large test before they went on to the 8-inch test. TLSGT is a slightly smaller LANL LSGT used only for TATB.

The early tests returned only the width of the spacer as the result. The U. S. Navy later measured the particle velocity in their spacers and determined a spacer pressure-distance calibration curve. For the modified gap test alone, they converted the spacer pressure into the inert explosive instant-of-impact pressure using impedance calculations. This was not done generally across all gap data, which far exceeds in quantity the flyer data.

We took the listed spacer pressure calibration as given by the Navy and the Air Force. All the earlier tests had to be modeled to get the pressure calibration curve. The next step is to convert the spacer pressures into pressures in the unreacted explosive upon impact, as was done first for the Navy's modified gap test. We have here extended this to all the tests, using the impedance method as described in Cooper

[26]. We take the spacer U_s-u_p coefficients and the particle velocity to be C_f, S_f and u_f. The same in the unreacted explosive are C_o, S_1 and u_p. We know the pressure in the space material, which we convert to spacer particle velocity, u_f, using

$$P(spacer) = \rho_f C_f u_f + \rho_f S_f u_f^2 \tag{12}$$

In the quadratic solution for u_f,

$$u_f = \frac{-b \pm (b^2 - 4ac)^{1/2}}{2a} \tag{13}$$

a = $\rho_f S_1$, b = $\rho_f C_o$ and C = -*P*. Next we calculate the explosive pressure. At the instant of impact, these pressures are the same:

$$P(explosive) = \rho_o C_o u_p + \rho_o S_1 u_p^2 = \rho_f C_f \left(2u_f - u_p\right) + \rho_f S_f \left(2u_f - u_p\right)^2 . \tag{14}$$

We solve this quadratic equation using Eq. (13) where

$$\begin{aligned} a &= \rho_f S_f - \rho_o S_1 \\ b &= -\rho_f C_f - 2\rho_f S_f (2u_f) - \rho_o C_o \\ c &= \rho_f C_f (2u_f) + \rho_f S_f (2u_f)^2 \end{aligned} . \tag{15}$$

Using this, we can calculate the explosive pressure. The unreacted U_s-u_p coefficients of explosives are available for the common dense ones. Many are not measured, but we use this overall estimation procedure:

$$\begin{aligned} &C_o(mm/\mu s) \approx 0.44\rho_o^3; \quad Co \le 2.4 \\ &C_o(mm/\mu s) \approx 2.4 \quad high \ \ values \\ &S_1 = 2 \end{aligned} . \tag{16}$$

The results are not sensitive to small errors in these coefficients. The U_s-u_p coefficients of the spacer materials are given in Table 2.

As a shock wave moves farther into a spacer, the peak pressure will continuously decrease, yet the gaps are small in the SSGT's and large in the Eglin tests. The reason for this is shown in Figure 1, where

the distance into the spacer is divided by the explosive donor radius listed in Table 1. The Y-axis is the calculated explosive pressure for LX-17 at 1.90 g/cm^3 with $C_o = 2.4$ and $S_1 = 2$. This dimensionless plot brings all the curves fairly close together and conceptually unifies the gap tests. Bigger tests will require larger gaps to prevent detonation in the acceptor. The measured and calculated gaps for the SSGT's have the most error for this reason.

The explosive pressure is not solely a function of donor radius because some tests are unconfined and some are not. In Figure 2, we show two near-ideal explosives with the explosive pressures plotted in descending order. This order is

LANL SSGT > LANL LSGT > NSWC SSGT > NSWC LSGT>ELSGT>Eglin 8-inch, (17)

which roughly tracks the donor radius. Table 3 lists more comparative results where three or more gap tests were run on the same explosive in a narrow density range [16, 21, 23-25, 27]. The small and large scale tests at LANL and LSGT form the most common set. The top section contains near-ideal explosives, where the calculated pressures decrease in the order of Eq. (17). The last four entries are non-ideal and the order changes because of the size effect on non-ideal explosives. A good example is TATB, which has an out-of-order value of 33 GPa for the NSWC SSGT but only 14 GPa for the LANL SSGT. The former has a acceptor radius of only 2.55 mm so that the detonation is near failure, but the latter has a 6.5 mm radius. If the radius is too small, the detonation cannot propagate at all.

In order to better describe non-ideal explosives, we next calculated the time widths at half-height of the pressure pulses in the spacer materials using JWL++ [28] for the donor explosives. We would expect that the time width of the spacer pulse would increase with increasing distance, just as the pressure decreases. The calculated results are shown in Figure 3, and we see that peaks occur. The distance into the spacer increases from right to left, so that the time widths generally increase but suffer a decrease when the rarefactions arrive from the sides.

Next, in Figure 4, we plot the pressure-time results for LX-17 and PBX 9502 at 1.88-1.90 g/cm^3. The flyer data is the P^2-τ result, where the time is the actual pulse length in the explosive [29]. The gap test data uses the spacer time widths, which empirically work as a proxy for actual pulse time because the two are roughly the same. The important thing is that the gap test data is seen to provide points along the P^2-τ curve, even if they are not as well characterized. In order to get the asymptotic pressure threshold, we need very thick flyers, which usually never get. The Eglin tests are so large that they provide a direct measure of this special threshold.

4 Pressure Threshold Summary

Now we summarize the results most likely to give P_o pressure thresholds. In Table 4, we pull together the three sources of pressure data: flyer thresholds [3, 6, 29-34], calculated run-time values [24, 33, 35-42] and the smallest gap test pressures available [18, 21]. The flyer data is clearly the best, because the pulse is well-characterized. The run-to-detonation is the worst because the threshold pressure is obtained by a complicated fit of the data. Yet the threshold is there and can be had as part of the sensitivity study that prompted the run experiments. The small gap tests give high-pressure thresholds as we would get with thin flyers, but the gaps are small, the tests are uncharacterized and the calculations have high errors. The Eglin gap tests are excellent because they give almost directly the asymptotic pressure thresholds. The NSWC LSGT are big enough and well characterized so that their thresholds are close to being asymptotic. A much wider range of materials have been run with this test, so that it constitutes the broadest repository of useful initiation data.

It is natural to take certain values as being near the asymptotic ones even though they probably are not. An important trend is that such thresholds increase with density as seen in Figure 5. For TATB and TATB/up-to-15% kel-F, the "asymptotic" pressure may be fit using

$$P_O(TATB,GPa) \approx 1.63x10^{-4}\, exp(5.73\rho_O),\quad 1.70 < \rho_O < 1.91\ \ g/cm^3. \tag{18}$$

So we predict asymptotic thresholds of 4.9 GPa at 1.80 g/cm^3 and 8.7 GPa at 1.90 g/cm^3. Figure 5 is divided first into pure TATB and TATB/binder with the high-TATB explosives LX-17, PBX 9502, T1, T2 and T3. There is no difference between the two. The points are also broken into the type of test, and again, there is no difference, even the flyer is considered better than the run-to-detonation.

In summary, one criticism of gap tests as being "not meaningful" hinges on the previous inability of the data to be compared [14]. However, we find that the gap tests constitute a previously unused repository of threshold information, which becomes comparable by converting all the gap data into explosive pressures and spacer pulse times. The addition of the flyer and run-time data unifies the pressure thresholds into a large body of data.

5 References

[1] F. E. Walker and R. J. Wasley, Critical Energy for Shock Initiation of Heterogeneous Explosives, *Explosivestoffe,* **1969,** *17*, 9-13.

[2] P. W. Cooper, *Explosives Engineering*, Wiley-VCH, New York, **1996**, pp. 310-312.

[3] Y. de Longueville, C. Fauquignon and H. Moulard, Initiation of Several Condensed Explosives by a Given Duration Shock Wave, *Proceedings Sixth Symposium (International) on Detonation*, Coronado, CA, August 24-27, **1976**, pp. 105-114.

[4] H. R. James, An Extension to the Critical Energy Criterion used to predict Shock Initiation Thresholds, *Propellants, Explosives, Pyrotechnics,* **1996,** *21*, 8-13.

[5] J. Roth, Shock Sensitivity and Shock Hugoniots of High-Density Granular Explosives, *Proceedings Fifth Symposium (International) on Detonation*, Pasadena, CA, 18-21 August, **1970**, pp. 219-230.

[6] LeRoy Green, Lawrence Livermore National Laboratory, private communication, **2005**.

[7] G. H. Bloom, Flash Threshold of Shocked Aluminum Silicofluoride, Lawrence Livermore National Laboratory report UCID-21259 (**1987**).

[8] Chadd May, Roy Hanks, Ralph Hodgin and Henry Chau, Experimental Determination of the James Initiation Parameters for LX-16, to be submitted, *Propellants, Explosives, Pyrotechnics*.

[9] Physical Testing of Explosives, U. S. Dept. of Commerce, Bureau of Mines, Bulletin No. 346 (**1931**).

[10] G. Herzberg and G. R. Walker, Optical Investigations of Initiation and Detonation, I, II, III. Project XR-84. Dept. of Physics, Uni. Of Saskatchewan, March, **1945**-August, **1946**.

[11] G. Herzberg and G. R. Walker, Initiation of High Explosives, *Nature (London), 1948,* **161**, 647-648.

[12] C.-O. Leiber, Assessment of Safety and Risk with a Microscopic Model of Detonation, Elsevier, New York, **2003**, pp. 75-76, 239.

[13] G. F. Miller and H. Pursey, On the Partition of Energy between Elastic Waves in a Semi-Infinite Solid, *Proc. Royal Soc.,* **1955***, A233*, 55-69.

[14] Reference 12, pp. 219-238.

[15] R. B. Frey and J. J. Trimble, Nondetonative Transitions in Confined Explosive Charges, *Proceedings Seventh Symposium (International) on Detonation*, Annapolis, MD, 16-19 June, **1981**, pp. 247-255.

[16] J. C. Foster, Jr., K. R. Forbes, M. E. Gunger and B. G. Craig, An Eight-Inch Diameter, Heavily Confined Card Gap Test, *Proceedings Eighth Symposium (International) on Detonation*, Albuquerque, NM, July 15-19, **1985**, pp. 229-236. The Eglin very large geometries are on pp. 230.

[17] S. A. Aubert, G. H. Parsons, J. G. Glenn and J. L. Thoreen*, Calibration and Correlation of a Modified Expanded Large Scale Gap Test with the Small Scale Gap Test and the 8-inch Gap Test*, Air Force Armament Lab, Eglin AFB, FL, report AFATL-TR-89-46; ADB-137016, August, **1989**. The ELSGT geometry is on pp. 2, 4, 7-9.

[18] S. A. Aubert, G. H. Parsons, J. G. Glenn and J. L. Thoreen, Gap Tests as a Method of Discriminating Shock Sensitivity, *Proceedings Ninth Symposium (International) on Detonation,* Portland, OR, August 28-September 1, **1989**, pp. 1284-1293. The ELSGT geometry is on p. 1286.

[19] T. P. Liddiard and J. W. Forbes, Initiation of Burning and Detonation in Cast H-6 and Cast PBXW-109, *Proceedings Seventh Symposium (International) on Detonation*, Annapolis, MD, 16-19 June, **1981**, pp. 308-314. The MGT geometry is on p. 309.

[20] J. W. Forbes, J. W. Watt and H. D. Adolf, *The Insensitive High Explosives (IHE) Gap Test,* Naval Surface Weapons Center, Dahlgren, VA, report NSWC TR-86-58, AD-B-111475, July, **1986**. The IHEGT geometry is on p. A-2.

[21] D. Price, A. R. Clairmont, Jr. and J. O. Erkman, *The NOL Large Scale Gap Test. III. Compilation of Unclassified Data and Supplementary Information for Interpretation of Results*, Naval Ordnance Laboratory, White Oak, MD, report NOLTR 74-40, AD 780429, March, **1974**. The NSWC LSGT geometry is on p. 4.

[22] D. Price and T. P. Liddiard, Jr., *The Small Scale Gap Test: Calibration and Comparison with the Large Scale Gap Test*, Naval Ordnance Laboratory, White Oak, MD, report NOLTR 66-87; AD-487353, July, **1966**. The NSWC SSGT geometry is on p. 2.

[23] J. N. Ayres, L. J. Montesi and P. J. Bauer, *Small-Scale Gap Test (SSGT Data Compilation: 1959-1972. Volume I, Unclassified Explosives*, Naval Ordnance Laboratory, White Oak, MD, report NOLTR 73-132; AD-773743, October, **1973**. The NSWC SSGT geometry is on p. 3.

[24] *LASL Explosive Property Data*, T. R. Gibbs and A. Popolato, eds, University of California, Berkeley, **1980**. The LANL LSGT and SSGT geometries are on p. 425.

[25] M. J. Urizar, S, W. Peterson and L. C. Smith, *Detonation Sensitivity Tests*, Los Alamos National Laboratory, report LA-7193-MS, April, **1978**. The LANL LSGT and TLSGT geometries are on p. 8.

[26] Reference 2, p. 213.

[27] P. E. Kramer, *Performance and Sensitivity Testing of TATB*, Mason & Hanger-Silas Mason Co., Amarillo, TX, report HMSMP-78-59, November, **1978**.

[28] P. Clark Souers, Steve Anderson, Estella McGuire and Peter Vitello, JWL++: A Simple Reactive Flow Code Package for Detonation, *Propellants, Explosives, Pyrotechnics*, **2000**, *25*, 54-58.

[29] C. A. Honodel, J. R. Humphrey, R. C. Weingart, R. S. Lee and P. Kramer, Shock Initiation of TATB Formulations, *Proceedings Seventh Symposium (International) on Detonation*, Annapolis, MD, June 16-19, **1981**, pp. 425-434. The Pantex gap geometry is on p. 430.

[30] R. C. Weingart, R. K. Jackson, C. A. Honodel and R. S. Lee, Shock Initiation of PBX 9404 by Electrically-Driven Plates, *Propellants and Explosives,* **1980,** *5*, 158-162.

[31] C. Belanger, P. Pelletier and J. F. Drolet, "Shock Sensitivity Study of the Curable Plastic Bonded Explosives," *Proceedings Eighth Symposium (International) on Detonation,* Albuquerque, NM, July 15-19, **1985**, pp. 361-371.

[32] B. D. Trott and R. G. Jung, Effect of Pulse Duration on the Impact Sensitivity of Solid Explosives, *Proceedings Fifth Symposium (International) on Detonation*, Pasadena, CA, August 18-21, **1970**, pp. 191-204.

[33] R. K. Jackson, L. G. Green, R. H. Bartlett, W. W. Hofer, P. E. Kramer, R. S. Lee, E. J. Nidick, Jr., L. L. Shaw and R. C. Weingart, Initiation and Detonation Characteristics of TATB, *Proceedings Sixth Symposium International) on Detonation*, Coronado, CA, August 24-27, **1976**, pp. 755-765.

[34] J. P. Plotard, R. Belmas, M. Nicollet and M. Leroy, Effect of a Preshock on the Initiation of HMX, TATB and HMX/TATB Compositions*, Proceedings Tenth Symposium (International) on Detonation*, Boston, MA, 12-16 July, **1993**, pp. 507-514.

[35] J. B. Ramsay and A. Popolato, Analysis of Shock Wave and Initiation Data for Solid Explosives, *Proceedings Fourth Symposium (International) on Detonation,* White Oak, MD, October 12-15, **1965**, pp. 233-238.

[36] Unpublished data from Kevin Vandersall, Jerry Forbes, Paul Urtiew and Frank Garcia, Lawrence Livermore National Laboratory, private communications, **2002-2005**.

[37] B. D. Trott and R. G. Jung, Effect of Pulse Duration on the Impact Sensitivity of High Explosives, *Proceedings Fifth Symposium (International) on Detonation*, Pasadena, CA, August 18-21, **1970**, pp. 191-204.

[38] M. van Thiel, *Compendium of Shock Wave Data, Sections A2-B*, Lawrence Livermore National Laboratory report UCRL-50108 rev. 1, vol. 2, June, **1977**.

[39]D. C. Dallman and J. Wackerle, Temperature-Dependent Shock Inititation of TATB-Based Explosives, *Proceedings Tenth Symposium (International) on Detonation,* Boston, MA, July 12-16, **1993**, pp. 130-138.

[40] R. L. Gustavsen, S. A. Sheffield, R. R. Alcon, J. W. Forbes, C. M. Tarver and F. Garcia, Embedded Electromagnetic Gauge Measurements and Modeling of Shock Initiation in the TATB Based Explosives LX-17 and PBX 9502, *Shock Compression of Condensed Matter-2001*, American Institute of Physics, **2002**, pp. 1019-1022.

[41] J. J. Dick, C. A. Forest, J. B. Ramsay and W. L. Seitz, The Hugoniot and Shock Sensitivity of a Plastic-Bonded TATB Explosive PBX 9502, *J. Appl. Phys.,* **1988***, 63*, 4881.

[42] G. E. Seay and L. B. Seely, Jr., Initiation of a Low-Density PETN Pressing by a Plane Shock Wave, *Third Symposium on Detonation,* Princeton, NJ, September 26-28, **1960**, pp. 562-573.

Acknowledgement

This work was performed under the auspices of the U.S. Department of Energy by the University of California, Lawrence Livermore National Laboratory under Contract No. W-7405-Eng-48.

Table 1. Summary of gap test geometries.

		Donor					Acceptor	
No.	Lab & test	Radius (mm)	Explosive	Density (g/cm^3)	Length (mm)	Spacer	Radius (mm)	Length (mm)
1	LANL SSGT	3.81	PBX 9407	dense	5.26	Brass	6.35	50.8
2	Pantex	12.7	LX-04	1.86	38.1	Brass	12.7	25.4
3	LANL TLSGT**	12.7	PBX 9205	dense	101.6	Al dural	12.7	101.6
4	LANL LSGT	20.64	PBX 9205	dense	101.6	Al dural	20.64	101.6
5	NSWC SSGT	2.55*	RDX	1.56	36.3	Lucite	2.55	38.1
6	NSWC LSGT	25.4*	pentolite	1.56	50.8	Lucite	18.25	139.7
	NSWC IHEGT	25.4*	pentolite	1.56	50.8	Lucite	6.35	50.8
	NSWC MGT	25.5	pentolite	1.56	51	Lucite	25.5	12.7
7	Eglin ELSGT	47.62*	Comp B	1.38	95.25	Lucite	47.62	279.4
8	Eglin 8-inch	88.9*	Comp B	1.68	203.2	Lucite	88.9	?
9	Eglin Super 8-in. Flyer	90.81*	Comp B	1.68	203.2	Lucite	90.81	406.4

*confined acceptor ** for TATB only

Table 2. Densities and U_s-u_p coefficients for the gap test spacers.

	ρ_f (g/cm^3)	C_f (mm/μs)	S_f (dimless)
Lucite	1.182	2.18	2.088
Aluminum	2.707	5.39	1.34
Brass	8.45	3.726	1.434

Table 3. Comparison of measured threshold explosive pressures for 50% probability of detonation in gap tests. The top section is near-ideal; the two bottom sections are less ideal.

		Impedance-Calculated Explosive Pressures, P (GPa)					
	Density	LANL	LANL	NSWC	NSWC	Eglin	Eglin
	(g/cm^3)	SSGT	LSGT	SSGT	LSGT	ELSGT	8-inch
Amm Picrate	1.59-1.60	12	6		4		
Amm Picrate	1.64	12	6		4		
Comp A-3	1.61-1.62	9	4		1.5		
Comp A-3	1.64-1.65	11	4-5		1.7		
Comp B, cast	1.68-1.73	12	6-7		2-5	1.1	1.0
DATB	1.70-1.71	12	6	6	5		
DATB	1.78-1.79	13	8	7			
LX-04	1.83-1.86	11-13	5-6	3	4		
PBX 9404	1.77-1.79	9-10	4		4		
PBX 9407	1.65-1.66	6-7	4		2		
PBX 9407	1.76-1.77	10	5		3		
Pentolite, psd	1.66-1.68	9	2.3	1.4	1.1-1.6		
RDX	1.72-1.73	7	3	2			
Tetryl	1.62	12	5	1.5	1.3		
Tetryl	1.68-1.69	7-8	3.5	1.6			
TNT, pressed	1.57-1.58	11	4.5	2.6	2.3	2.0	1.7
TNT, pressed	1.62-1.65	12	5-6	3.4	2.9		
Tritonal	1.71-1.79		14		3-7	2.4	1.7
Baratol, cast	2.6	no det	12-15		7		
NQ	1.61-1.63	no det	17		9-10		
TATB	1.87-1.89	14	14	33	8		
	Density		LANL			Eglin	Eglin
Explosive	(g/cm^3)	Pantex	TLSGT			ELSGT	8-inch
PBX 9502	1.88-1.90	16-17	22			8.8	8.2

Table 4. Comparison of possible near-asymptotic pressure thresholds, P_o, from three sources: flyer, run-time and the lowest gap test, which is usually the NSWC LSGT. The asterisk indicates that the data is from the Eglin 8-inch gap test.

Explosive	Density (g/cm^3)	Pressure P_o (GPa) Flyer	Run-Time	Gap Test
RDX with cast TNT				
Comp B mil	1.69			2.1
Comp B mil	1.70		3.0	2.0
Cyclotol	*1.70*			2.8
Comp B mil	1.71			4.9
Comp B-3	1.71			2.1
H-6	1.75			3.7
HBX-3	1.85			5.1
Pressed TNT				
TNT	1.07			0.6
TNT	1.25			1.1
TNT	1.32			1.2
TNT	1.33			1.2-1.3
TNT	1.42			1.6
TNT	1.49			1.8
TNT	1.58			2.1-2.3
TNT	1.60			2.6
TNT	1.63		3.5	
TNT	1.64			2.9
TNT	1.65			1.7*
Cast TNT				
TNT	1.56			6.0-6.1
TNT	1.58			4.2
TNT	1.59			4.8
TNT	1.60			3.4
TNT	1.61			4.8-5.1
TNT	1.62			5.2-9.8
TNT	1.63		6.5	5.2
PETN				
PETN	1.00		0.22	
PETN	1.40		0.37	
PETN	1.60		1.0	
PETN	1.73		1.0	
Tetryl				
Tetryl	1.30		0.3	
Tetryl	1.40		0.45	
Tetryl	1.43			0.8
Tetryl	1.49			1.0
Tetryl	1.50		0.6	
Tetryl	1.60		1.0	
Tetryl	1.62			1.3

Explosive	Density (g/cm^3)	Pressure P_o (GPa) Flyer	Run-Time	Gap Test
HMX pbx's				
PBX 9404	1.70		1.1	
PBX 9404	1.77			3.9
HMX 89.5/ny	1.77	0.2		
PBX 9501	1.82		1.9	
X1 (HMX 96)	1.82		3.3	
LX-03-0	1.83			2.9
PBX 9404	1.84	1.5	1.9	
EDC-37	1.85		1.5	
LX-04-0	1.85		2.9	3.8
RDX, pressed pbx's				
A-3	1.40			1.2
C-4	1.41			1.5
A-3	1.45			1.5
CH-6	1.45			0.7
A-3	1.50			1.4-1.5
RDX	1.53			0.7
RDX	1.54	0.1		
A-3	1.55			1.4
C-4	1.56			2.3
CH-6	1.57			0.8
A-3	1.59			1.9
A-3	1.60			1.8
Comp C-3	1.60			2.5
CS-84A	1.60	0		
RDX 86/pb	1.60	1.0		
PBX 9407	1.60		1.1	
A-3	1.61			1.5
RDX	1.64			0.8-1.1
A-3	1.65			1.7
A-3	1.68			1.4
CH-6	1.70			1.3
TATB, pure and High % pbx's				
TATB	1.69			3.5
PBX 9502	1.70	3.5		
TATB	1.70	2.0		
PBX 9502	1.80	4.5		
TATB	1.80	4.5		
TATB	1.81		5.0	
TATB	1.82			7.9
T2	1.855		9.5	

Tetryl	1.64		1.6
Tetryl	1.70	2.1	
Ammonium Perchlorate, 7-11 µm			
AP	0.80		1.0
AP	1.07		1.6-1.7
AP	1.17		2.1
AP	1.25		2.1
AP	1.27		2.4-2.6
AP	1.31		2.5
AP	1.38		3.3
AP	1.43		4.3
AP	1.46		4.7-5.0
AP	1.52		6.1
AP	1.56		6.7-6.9
AP	1.57		6.8-7.2

PBX 9502	1.88	6.0		
T1	1.89	8.5	8.5	
PBX 9502	1.89			8.2*
T2	1.90	10	8.0	
X-0219	1.90		8.5	
LX-17 Green	1.90	8.0	9.5	
LX-17 no Green	1.90	9.5	9.5	
PBX 9502	1.90		7.0	
T3	1.91	12	10.0	
X-0219	1.92		11.0	
TATB 85/ kel-F	1.93		12.5	

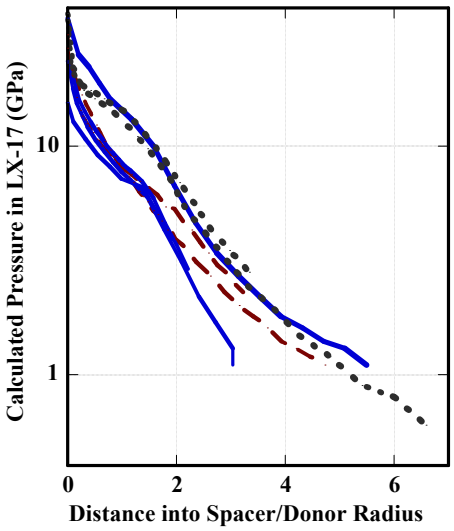

Figure 1. Comparison of calculated pressures in LX-17 for all tests, where distance into the spacer is dimensionless. The lines are: full -Lucite, dashed- brass and dotted-aluminum.

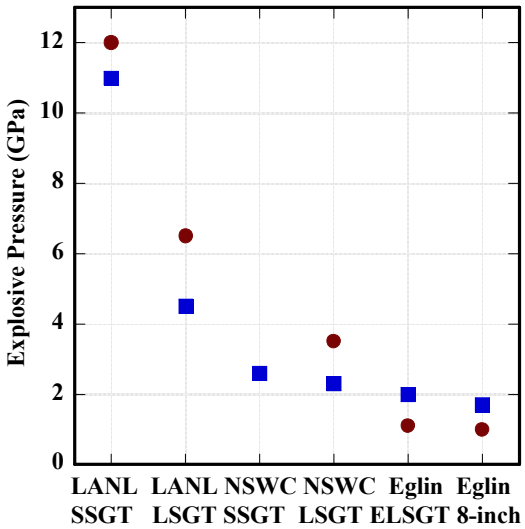

Figure 2. Pressure in the spacer material in six gap tests for cast Comp B (circles) and pressed 1.57-1.58 g/cm^3 TNT (squares).

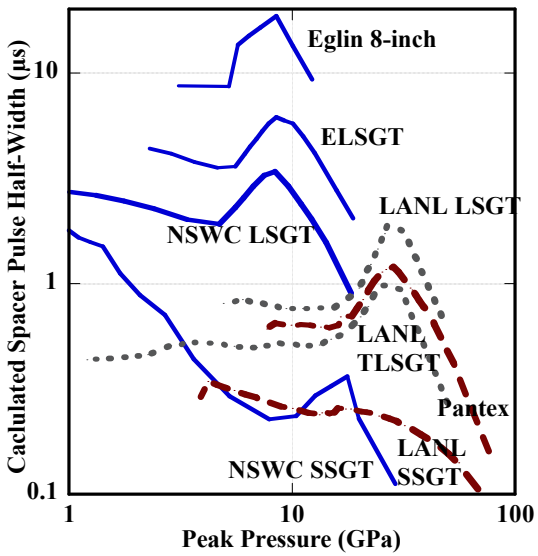

Figure 3. Pulse time widths in the spacers as a function of pressure. Distance increases in the spacer as we move from right to left.

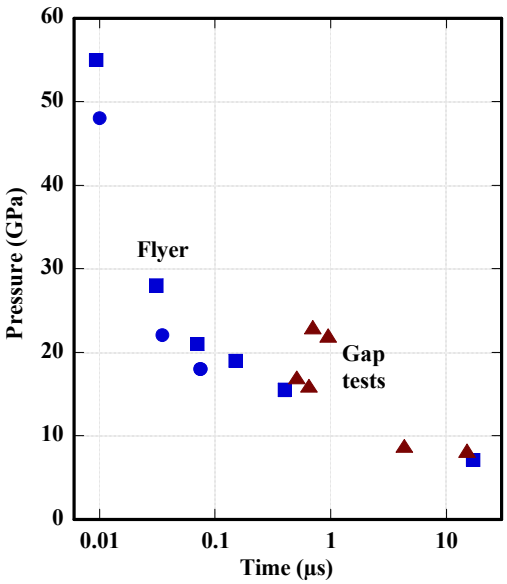

Figure 4. Pressure-time curve for flyer and gap test data for LX-17 and PBX 9502 at 1.88-1.90 g/cm^3. For flyers (LX-17-squares; PBX 9502-circles), the time is the pulse length in the explosive as calculated from the flyer thickness. For gap tests (PBX 9502-triangles), it is the time width in the spacer at the point of 50% detonation probability.

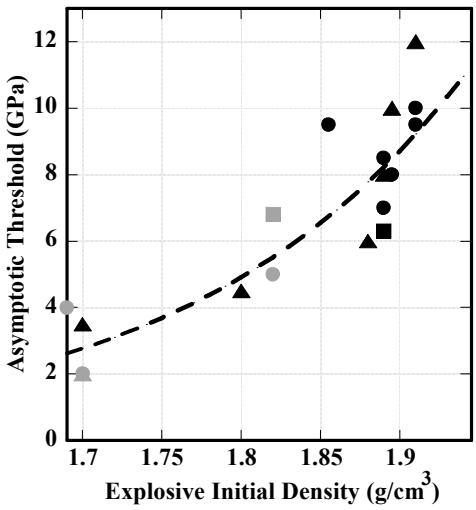

Figure 5. Asymptotic pressure thresholds as a function of density for pure TATB (gray) and TATB /binder (black). The tests are: flyer (triangles), run-to-detonation (circles) and gap test (squares). The dashed line is the fit.